ELSEVIER

Chemical Engineering Journal 70 (1998) 125–131

Chemical Engineering Journal

Simulation and optimisation of intermittent membrane microfiltration

E.J. Farley *, D.A. White

Department of Chemical Engineering, Imperial College, London SW7 2BY, UK

Received 11 November 1997; accepted 2 March 1998

Abstract

Cyclical stop–start operation as a method of increasing permeate production and lowering energy requirements is discussed. It is thought that the removal of the applied pressure allows the reversible fouling, such as concentration polarisation, to dissipate. A model to simulate intermittent operation is developed and optimised with respect to optimising the permeate production. The model was used to simulate a theoretical optimised run and the results compared to those obtained from experiment. The experiments were performed with a dilute suspension of magnesium hydroxide and a range of cross-flow velocities. The experimental results were in good agreement with those calculated from the theoretical model. The use of intermittent operation showed permeate production increases in the order of 200% when compared to the permeate production of a steady flow run. Energy savings of more than 50% are also reported when using intermittent operation.

Keywords: Simulation; Optimisation; Membrane microfiltration

1. Introduction

Continuous membrane filtration operation is characterised by constant transmembrane pressure and cross-flow velocity throughout the experimental runtime apart from the initial falling rate period which is of comparatively small duration. In the steady-state period, the particles that are moving towards the membrane surface, due to convective drag effects, are in equilibrium with those being swept out of the membrane due to the shearing effect of the flow. This keeps the fouling layer thickness constant, hence keeping the resistance to flow through the membrane steady [1]. The value of the permeate flow in this region has been donated as the steady-state permeate flow rate, f_s (m/s).

It has been well documented that a fundamental reason for flux decline in membrane filtration systems is a concentrated layer of particles forming above the membrane surface [2,3]. This particle layer, sometimes referred to as the concentration polarisation layer, forms due to the connective drag force towards the membrane surface induced by the direction of the permeate flow. The concentration polarisation layer differs from a physical fouling layer, as it is reversible while a physical fouling layer is not. If the concentration polarisation layer can be reduced or dislodged, then the resistance is reduced and the permeate flow increased. Methods of disturbing the formation of this concentration layer are often referred to as 'flux enhancement techniques'.

When air is injected directly into the feed stream complex hydrodynamic conditions are set up within the membrane module due to the resulting slug flow. This disrupts the concentration layer formation and flux improvements of 200% have been reported for the ultrafiltration of bentonite and yeast through a tubular mineral membrane [4]. Unsteady flow can be obtained without altering the feed, by the use of a pulsation generator [5]. This was obtained by using a collapsible tube, which introduced a pulsatile component to the steady flow. Flux improvements of up to 60% were reported for the microfiltration of a dilute suspension of silica particles through a tubular ceramic membrane. Flux enhancement by the insertion of baffles or static mixers, as turbulence promoters, has been reported by several workers [6,7], and flux enhancements of around 50% were found for the ultrafiltration of a 3% dextran solution using a cellulose acetate membrane.

The techniques of using oscillatory flow combined with static mixers has been employed to create a vortex wave that increases shearing at the membrane surface, and hence disrupting the concentration layer. Enhancements of up to 350% were found for the ultrafiltration of blood plasma in laminar flow [8].

Other methods of flux enhancement exist, which do not directly deal with the formation of the concentration layer.

* Corresponding author.

1385-8947/98/$19.00
PII S1385-8947(98)00087-4

The use of filter additives, such as diatomaceous earth and polymeric flocculants, have been used to reduce the compressibility of the cake layer forming on the membrane surface. In dead end, vacuum filtration flux improvements of 350% have been reported [9] and in the continuous filtration of bentonite clay, initial flux improvements of 300% have been reported [3]. Pretreatment of a polysulfone ultrafiltration membrane with a surfactant has shown flux improvement in the order of 80% which rose to almost double when an 'anti-foam' agent was also added to the feed [10].

Intermittent operation has been reported by several workers previously, but with important differences. Si-Hassen et al. [11] used a test solution of $CaCO_3$, at a concentration of 100 g/l, and imposed cleaning phases by removing the transmembrane pressure but circulating the test solution at 4 m/s. To perform the filtration, the transmembrane pressure was raised to an average value of 3.2 bar and the cross-flow velocity lowered to 0.5 m/s. The results were compared to a steady run on the basis of hydraulic energy consumption. It was reported that in intermittent operation, there is substantial hydraulic energy savings.

Xu et al. [12] reported a discontinuous microfiltration process using dead-end filtration of fine particles. Although the theory, which is based on Darcy's law, is for dead-end filtration, the authors suggest a possible extension to cross-flow microfiltration. The cleaning phase for this process is achieved by periodic backwash of the permeate and occasional chemical treatment.

White and Lesecq [13] modeled intermittent operation as a series of cycles. In between the cycles, the applied pressure to the membrane is removed. At this time, any reversible fouling, such as concentration polarisation, dissipates. In this case, it is more difficult to calculate the average permeate flow than it is in continuous operation. A typical time vs. permeate flow graph for intermittent operation is shown in Fig. 1.

It can be seen from this figure that the permeate flux 'recovers' when the pump is switched back on again; however, the magnitude of the initial flux at the beginning of each cycle decreases with time. White and Lesecq [13] proposed to model the flux rate change with time for each cycle of the intermittent run with time by the following equation:

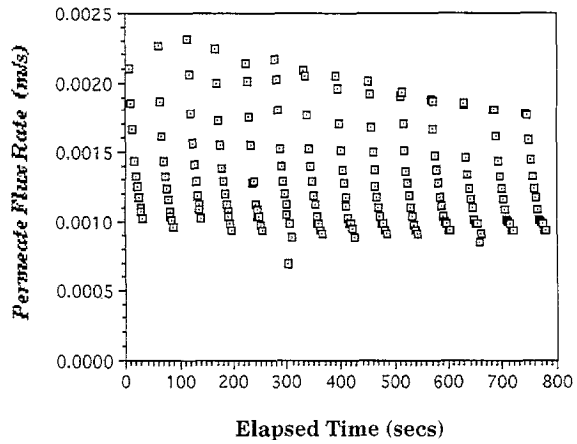

Fig. 1. Typical intermittent run.

$$f=f_0\left(\frac{t}{t_0}\right)^{-n} \tag{1}$$

In Eq. (1), t is the time since the start of the cycle, t_0 is the initial time at which the first reading of the cycle was made, and f_0 is the flux rate measurement at that point. Exploring the limits of Eq. (1) shows that as the time increases the flux rate will eventually fall to zero. However, the flux in a microfiltration process declines to a steady-state value. Eq. (1), therefore, needs to be modified to take into account this fall to a steady-state value; this can be done by using an exponential decay model of the form,

$$f/f_0=a+b\exp(-t/c) \tag{2}$$

This gives that at $t\to\infty, f/f_0\to a$. In this last expression, a, b and c are constants, f is the permeate flow rate, f_0 is the initial cycle permeate flow rate, and t is the time after the cycle starts. It can be seen that when the time increases towards infinity the permeate flow rate falls to a constant value.

2. Intermittent operation model development

The form of Eq. (2) is more suitable for optimisation as it predicts a steady state period. The total permeate volume for a cycle of duration T seconds can be expressed as $p=\int_0^T f\cdot dt$. Here, p is the total permeate volume from time $t=0$ to $t=T$. The time T is the time that the membrane is actually running under cross-flow conditions; integration of Eq. (2) over the boundary limits stated gives,

$$p_n=f_0[aT_n+bc-bc\exp(-T_n/c)] \tag{3}$$

where p_n is the total permeate flow through the membrane for that particular cycle n.

Eq. (3) allows the mean permeate flow for each cycle to be calculated from

$$\bar{f}=\frac{p_n}{T_n+\theta}=\frac{p_n}{T_N} \tag{4}$$

Here, θ is the time that the applied pressure on the membrane was removed or the time of the quiescent period. Using this last expression and substituting it into Eq. (3), the following relationship is obtained:

$$\bar{f}=\frac{f_0}{T_n}\left\{a(T_N-\theta)+bc-bc\exp\left(\frac{-(T_N-\theta)}{c}\right)\right\} \tag{5}$$

where $\bar{f}$ represents the average permeate flow rate for each cycle. The production of permeate for that cycle, p_n, can be expressed as $p_n=\bar{f}T_N$. The total production of permeate over the entire run, P_I, can be calculated from the expression $P_I=\sum_1^N[p_n]$ $n=1, 2, N$. This last expression allows a direct comparison of production rates with those calculated for continuous operation.

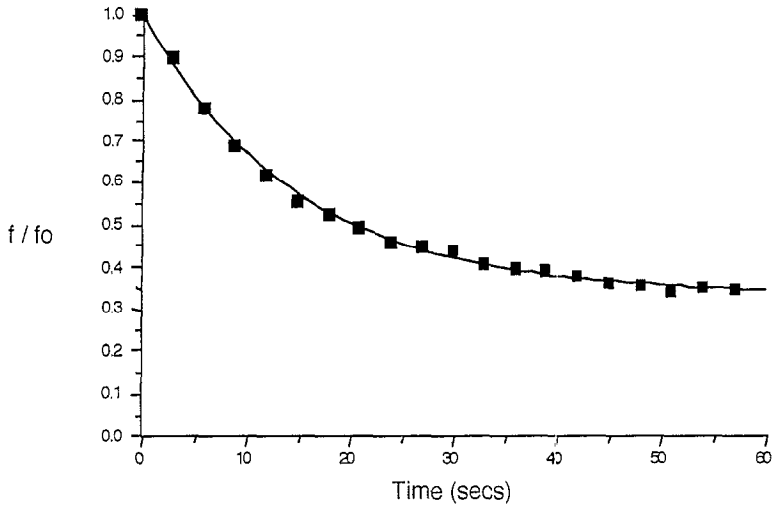

Fig. 2. Typical curve from microcal origin 4.1.

In the optimisation process, the value of the mean flux rate, which is given by $\bar{f}=(P_n)/(T+\theta)=(P_n)/(T_N)$, will be maximised. The magnitude of θ will be considered later. Rearranging the last expression gives

$$\bar{f}=\frac{f_0}{T+\theta}\left\{aT+bc-bc\exp\left(\frac{-T}{c}\right)\right\} \quad (6)$$

differentiating Eq. (6) with respect to T gives

$$\frac{d\bar{f}}{dT}=\frac{f_0}{(T+\theta)^2}\left\{\left[a+b\exp\left(\frac{-T}{c}\right)\right](T+\theta)-\left[aT+bc-bc\exp\left(\frac{-T}{c}\right)\right]\right\} \quad (7)$$

The mean flux is optimum when $(d\bar{f})/(dT)=0$. Substituting this into the last expression and rearranging for the optimum cycle time, T_{opt}, Eq. (8) is obtained.

$$T_{opt}=-c\ln\left\{\frac{bc-a\theta}{b(T_{opt}+\theta+c)}\right\} \quad (8)$$

Eq. (8) can be solved by simple iteration. The value for T_{opt} obtained can be used to calculate the optimal average permeate flow rate and consequently the optimal production rate. It should be noted that Eq. (8) is only valid when $\theta<(bc)/(a)$.

3. Experimental

The apparatus for determining the operational parameters for the simulation, a, b, c and f_0, has been described elsewhere [14]. The feed is pumped by a Jabsco 80 impeller pump. A valve has been installed that allows the feed to completely bypass the membrane module and return to the feed tank, in effect removing the applied pressure across the membrane.

Table 1
Typical correlation of a run

Cycle no.	Runtime (s)	a	b	c (s)
1	90	0.32	0.71	16.1
2	180	0.33	0.71	16.0
3	270	0.31	0.71	15.5
4	360	0.32	0.71	14.8
5	450	0.33	0.69	14.4
6	540	0.32	0.67	14.0
7	630	0.33	0.66	13.0

The relevant filtration data, transmembrane pressure, cross-flow velocity and the permeate flow rate are data logged via a microcomputer.

The data from the experimental apparatus data logging system was transferred to a curve fitting package produced by Microcal Software and called Microcal Origin 4.1. The parameters a, b, c and f_0 in Eq. (4) were determined for each individual cycle. This method of analysis proved to be rather time consuming, and Fig. 2 shows a typical graph obtained from the curve fitting package.

Table 1 shows the values obtained for a run where the time that pressure was applied to the membrane, T, was 60 s and the quiescent period was 30 s. The cross-flow velocity was 1.0 m/s, and the transmembrane pressure was 150 kPa. It can be seen that the values of a and b are constant and have a mean value of 0.32 and 0.70, respectively. The value of c decreases with time.

From the limits of Eq. (2) at time $t=\infty f/f_0=a$ and at time $t=0, f/f_0=a+b$. At the beginning of each cycle $f=f_0$, hence $a+b=1$, which is confirmed by the data in the table above.

4. Determination of the quiescent period

The aim of this section is to determine, from experiment, the minimum value of θ, the time that the applied pressure to

the membrane is removed. If the pressure is reapplied to the membrane rapidly also, then the reversible fouling such as concentration polarisation does not have sufficient time to disperse and the next cycle initial flux will be reduced significantly. The experimental apparatus was filled with a 0.2% by weight magnesium hydroxide slurry. Runs were carried out at 4 cross-flow velocities 0.5, 0.75, 1.25 and 1.65 m/s and 5 values of θ: 5, 10, 15, 20, and 30 s. Five seconds is practically the minimum value of the quiescent period to avoid overloading the pump. In each case, the apparatus was run for 1 min, to allow the fouling layers to become fully developed, and then stopped for the appropriate time and then started again. This was repeated for 10 min and the initial value of each cycle plotted against time. Typical results are presented in Figs. 3 and 4.

As can be seen from Fig. 3, the value of θ has a marked effect on the initial permeate flow of each cycle. As the quiescent period becomes smaller, so does the initial permeate flow, and this implies that the reversible fouling has not had sufficient time to dissipate, so the next cycle flux is impaired, so much so that at 10 s, the permeate flow after 5 min has fallen to virtually zero. At a cross-flow velocity of 0.5 m/s 30 s is the smallest value of θ for the dissipation of the reversible fouling.

Data for a higher cross-flow velocity of 1.25 m/s are shown in Fig. 4. These results are similar at all values of θ. The run

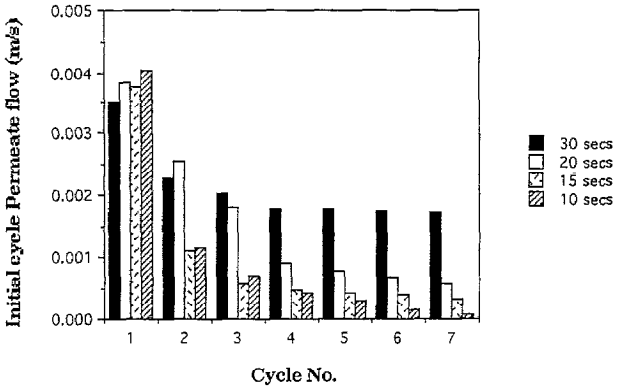

Fig. 3. Determination of the period of quiescence at a cross-flow velocity of 0.5 m/s.

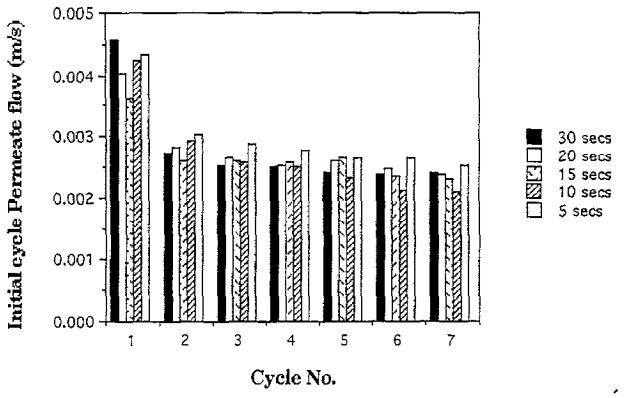

Fig. 4. Determination of the period of quiescence at a cross-flow velocity of 1.25 m/s.

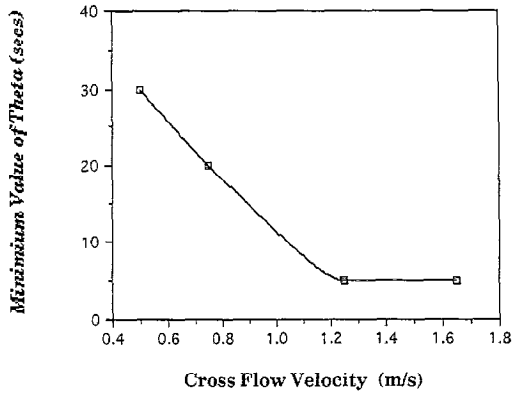

Fig. 5. Relationship between the cross-flow velocity and the period of quiescence.

when $\theta = 5$ s gives the highest values for the initial permeate flow, implying that the reversible fouling has dissipated even at the shortest value of θ under investigation. Data for the minimum value of θ for the different velocities studied are shown in Fig. 5. This figure shows that as the cross-flow velocity is increased, the minimum value for the period of quiescence is reduced.

A possible explanation of this is that at the higher cross-flow velocities the reversible fouling layer is being removed by the force of the flow when it is reintroduced to the membrane module. Whereas at the lower velocities (Fig. 3), the flow is not removing the concentration polarisation layer, it dissipates with time when the transmembrane pressure is removed. A concentration polarisation layer forms due to the convective drag effects of the permeate flow sweeping particles towards the membrane surface and back diffusion of the particles towards the bulk of the fluid. When the transmembrane pressure is removed, the permeate flow ceases but back diffusion will not; hence, the concentration layer dissipates.

5. Simulation of a filtration cycle

If the relationship of the initial cycle flux, f_0, and c to the total experimental runtime is known a simulation of a filtration cycle can be carried out. The relationships are determined experimentally and can be seen in Figs. 6 and 7. Fig. 6 shows, for a cross-flow velocity of 0.75 m/s, the relationship of the initial cycle permeate flow to the time that the membrane has been in operation. After the initial flux decline the initial cycle permeate flow follows a linear relationship; for the purpose of the simulation, the initial decline has been disregarded, and the linear relationship has been used.

Fig. 7 shows the relationship of the c parameter to the time that the membrane has been in operation. Although there is some scatter in the data, a linear relationship is an indication at all cross-flow velocities under consideration.

Using the information contained in Figs. 6 and 7, a spreadsheet was set-up that iterated Eq. (8) to a steady-value of the optimum cycle time for each cycle in the simulation. The

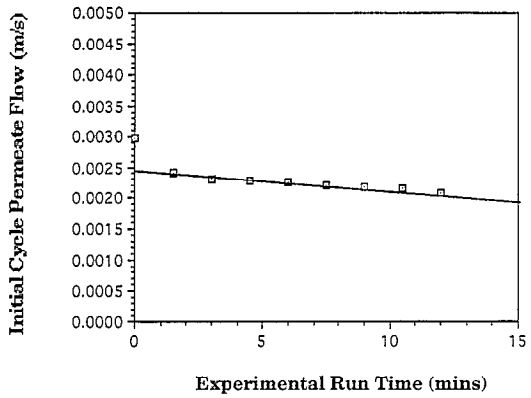

Fig. 6. Values of the initial cycle permeate flow for a cross-flow velocity of 0.75 m/s.

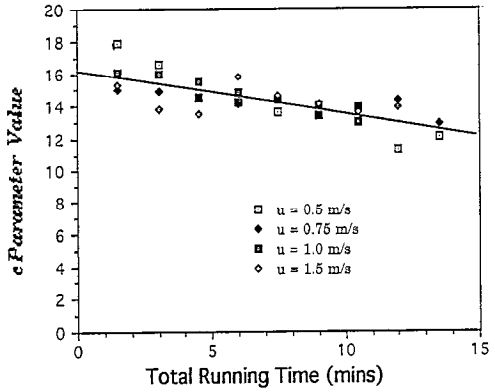

Fig. 7. Values of the c parameter.

values of a and b are fixed, and the duration of quiescence was obtained from Fig. 5. Using Eq. (4), the total volume of permeate for that cycle can be calculated. In this manner, a series of cycles that make up a filtration cycle can be calculated. The results for the filtration of 0.2% by weight slurry of magnesium hydroxide, with a cross-flow velocity of 0.75 m/s and a transmembrane pressure of 150 kPa, are presented in Table 2.

In this manner a production rate, P (m^3/m^2 s), for each cross flow velocity can be calculated from Eq. (9):

$$P=\frac{p_n A}{T_N} \tag{9}$$

where T_N is the total run time of the experiment and A is the membrane area in m^2. It should be noted that T_n is the time of a single cycle within the filtration experiment, whereas T_N is the total time of the filtration experiment.

Using the simulated data, such as that in Table 2, the experimental apparatus was run at the optimum cycle times determined for each cross-flow velocity. The minimum period of quiescence was determined, for each cross-flow velocity, from Fig. 5. The experimental runs were analysed in the same way as before, using Microcal Origin 4.1, and the production rate calculated from Eq. (4). Fig. 8 was then plotted, showing the simulated optimum production rate, the experimentally determined production rate using the

Table 2
Simulated results for a crossflow velocity of 0.75 m/s

Cycle no.	f_c (m/s)	c (s)	T_{Opt} (s)	p_n m^3	Time of cycle (s)
1	0.00243	14.9	40.6	0.0555	60.6
2	0.00239	14.7	40.6	0.0543	60.6
3	0.00234	14.5	40.6	0.0531	60.6
4	0.00230	14.3	40.7	0.0520	60.7
5	0.00226	14.1	40.7	0.0508	60.7
6	0.00222	13.9	40.8	0.0497	60.8
7	0.00218	13.7	40.9	0.0486	60.9
8	0.00213	13.5	41.1	0.0476	61.1
9	0.00209	13.3	41.2	0.0465	61.2
10	0.00205	13.1	41.4	0.0455	61.4
11	0.00201	12.9	41.6	0.0445	61.6
12	0.00196	12.7	41.8	0.0435	61.8
13	0.00192	12.5	42.1	0.0425	62.1
14	0.00188	12.3	42.5	0.0416	62.5
15	0.00184	12.1	42.9	0.0407	62.9

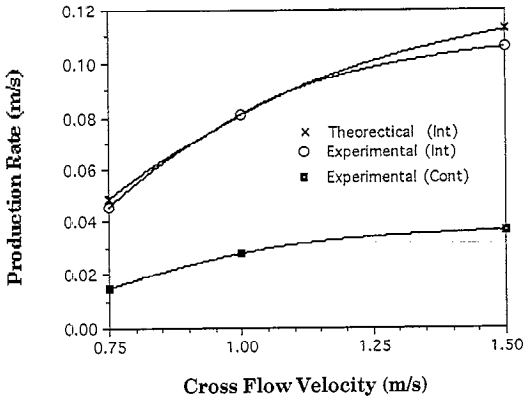

Fig. 8. Comparisons of theoretical and experimental results.

optimum cycle times, and for comparison, the equivalent steady operation production rate, which were experimentally determined.

6. Calculation of specific energy requirements

The production rate for steady operation, P_s (m^3), is the product of the mean flux, the time that the membrane module is in operation and the area of the membrane, A (m^2):

$$P_s=f_0 a(T+\theta)A \tag{10}$$

In Eq. (10), the mean flux is donated by f_0, which neglects the initial permeate flow decline. This assumption becomes valid after the first few cycles.

The energy input J_s (kJ) is the product of the amount of work put into pumping the feed stream around the apparatus and the time that the membrane is in operation.

$$J_S=E(T+\theta) \tag{11}$$

It should be noted that when direct comparisons are made between intermittent and steady operation, that when the

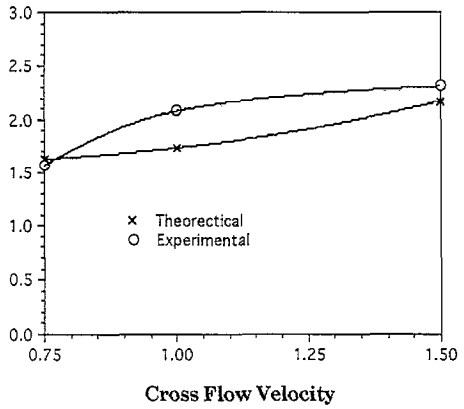

Fig. 9. Comparisons of energy requirements.

intermittent operation is at rest the steady operation is still running. This is why Eqs. (10) and (11) not only have the run time of a cycle, but also the quiescent period.

The production rate for intermittent operation can be determined from Eq. (4) multiplied by the area of the membrane in use.

$$P_I = f_0 A\{aT + bc - bc\exp(-T/c)\} \quad (12)$$

The energy consumed in intermittent operation is the product of the amount of work applied and the run time of the membrane.

$$J_I = ET \quad (13)$$

were E (kW) is the work required to pump the solution through the membrane module.

The specific energy requirement S (kJ/m^3), for both steady and intermittent flow can be expressed as energy consumed divided by the rate of production of permeate, $S = J/P$. Defining ϕ as the ratio of the specific energy requirements, $\phi = S_S/S_I$, and substituting Eqs. (10)–(13), the following relationship can be obtained:

$$\phi = \left\{1 + \frac{bc}{aT}[1 - \exp(-T/c)]\right\} \quad (14)$$

Eq. (14) allows a comparison between the energy requirements, if ϕ is greater than 1, then intermittent operation offers energy savings over steady operation. Fig. 9 shows the results, over the first 15 cycles, of a series of intermittent runs calculated at the optimum cycle times and at cross flow velocities of 0.75, 1.00 and 1.5 m/s.

7. Conclusions

Fig. 8 shows that the use of intermittent operation gives a substantial increase in the production of permeate when compared with continuous operation, in the order of 200%. As well as the increase in the permeate production, Fig. 9 shows that there is also a reduction in the specific energy requirements of intermittent operation, of up to 100% at the higher cross-flow velocities and 50% at the lower cross-flow velocities. This is due to the period of quiescence, where the energy consumed is assumed to be negligible as there is no pressure applied to the membrane. Practically, there would be several membrane modules in parallel and instead of switching the pump off, the feed would be diverted to another membrane module. This method of operation has two advantages, the first being that diverting the feed flow instead of switching the pump off saves wear and tear on the pump, and second, the modules that are not in operation can be dismantled and cleaned.

The use of intermittently operated membrane microfiltration, in the case described in this paper, has shown not only to dramatically increase the production of permeate, but to also reduce the amount of energy consumed. This is a great advantage over other methods of flux enhancement, as it utilises less power overall than the continuous process. Other methods of flux enhancement, such as air injection or the use of turbulence promoters, would require greater power and hence greater cost to achieve an increase in permeate production.

The filtration of $Mg(OH)_2$ slurry gives a superficial fouling layer where the particles do not enter the membrane structure. It should therefore be noted that the validity of the data is probably limited to cases of superficial fouling such as that encountered with the filtration of mineral suspensions of large particles. To confirm this, experiments using biological fluids and colloidal solutions should be performed.

The comparison of specific energy requirements in the operation of other flux enhancement techniques should be considered, and investigations into possible methods of industrial operation need to be carried out. Also, the sensitivity of the model to scaling up a single membrane tube into an industrial monolith needs to be examined.

8. Nomenclature

A	Membrane Area	m^2
a	Constant in Eq. (2)	
b	Constant in Eq. (2)	
c	Parameter in Eq. (2)	s
d	Internal Diameter of Membrane	m
E	Work required	kW
ΔP	Pressure drop along the membrane length	Pa
f	Permeate flow rate at time t	m/s
f_0	Initial permeate flow rate	m/s
f_s	Steady-state permeate flow rate	m/s
$\bar{f}$	Average permeate flow rate over time	m
J	Energy Input	kJ
n	Parameter in Eq. (1)	
θ	Quiescent period	s
p_n	Permeate flow of cycle n	m
S	Specific energy requirements	kJ/m^3 s
t	Time parameter in Eq. (2)	s

T	Actual time membrane is in operation	s
T_n	Total runtime of cycle n	s
T_N	Total runtime of the experiment	s
u	Cross-flow velocity	m/s
χ^2	Regression analysis from Origin 4.1	
ϕ	Ratio of specific energies	

References

[1] A.S. Michaels, New separation technique for the CPI, Chem. Eng. Prog. 64 (1968) 31–43.

[2] H. Strathman, Membrane separation processes, J. Membr. Sci. 9 (1981) 121–189.

[3] M. Mietton Peuchot, R. Ben Aim, Improvement of crossflow microfiltration performances with flocculation, J. Membr. Sci. 68 (1992) 241–268.

[4] M. Mercier, C. Fonade, C. Lafforgue-Delorme, How slug flow can enhance the ultrafiltration flux in mineral tubular membranes, J. Membr. Sci. 128 (1997) 103–113.

[5] C.D. Bertram, M.R. Hoogland, H. Li, R.A. Odell, A.G. Fane, Flux enhancement in crossflow microfiltration using a collapsible-tube pulsation generator, J. Membr. Sci. 84 (1993) 279–292.

[6] E.W. Pitera, S. Middleman, Convection promotion in tubular desalination membrane, Ind. Eng. Chem. Process Des. Dev. 12 (1973) 52.

[7] V. Mavrov, N.D. Nikov, M.A. Islam, J.D. Nikolova, An investigation on the configuration of inserts in tubular ultrafiltration module to control concentration polarisation, J. Membr. Sci. 75 (1992) 197–201.

[8] H.R. Millward, B.J. Bellhouse, I.J. Sobey, R.W.H. Lewis, Enhancement of plasma filtration using the concept of the vortex wave, J. Membr. Sci. 100 (1995) 121–129.

[9] C.W. Suh, S.E. Kim, E.K. Lee, Effects of filter additives on cake filtration performance, Korean J. Chem. Eng. 14 (1997) 241–244.

[10] K. Yamagiwa, H. Kobayashi, M. Onodera, A. Ohkawa, Y. Kamiyama, K. Tasaka, Surfactant pretreatment of a polysulfone ultrafilter for reduction of anti-foam fouling, Biotechnol. Bioeng. 43 (1994) 301–308.

[11] D. Si-Hassen, A. Ould-Dris, M.Y. Jaffrin, Y.K. Benkahla, Optimisation of an intermittent cross-flow filtration process of mineral suspensions, J. Membr. Sci. 118 (1996) 185–198.

[12] Y. Xu, J. Dodds, D. Leclerc, Optimisation of a discontinuous microfiltration-backwash process, Chem. Eng. J. 57 (1995) 247–251.

[13] D.A. White, P. Lesecq, Optimisation of intermittently operated microfiltration processes, Chem. Eng. J. 52 (1993) 73–77.

[14] M. Asaadi, D.A. White, A model for determining the steady state flux of inorganic microfiltration membranes, Chem. Eng. J. 48 (1992) 11–16.